LETTERS

Distinct sensory representations of wind and near-field sound in the *Drosophila* brain

Suzuko Yorozu[1,2], Allan Wong[1,2], Brian J. Fischer[1], Heiko Dankert[1,3], Maurice J. Kernan[4], Azusa Kamikouchi[5,6], Kei Ito[5] & David J. Anderson[1,2]

Behavioural responses to wind are thought to have a critical role in controlling the dispersal and population genetics of wild *Drosophila* species[1,2], as well as their navigation in flight[3], but their underlying neurobiological basis is unknown. We show that *Drosophila melanogaster*, like wild-caught *Drosophila* strains[4], exhibits robust wind-induced suppression of locomotion in response to air currents delivered at speeds normally encountered in nature[1,2]. Here we identify wind-sensitive neurons in Johnston's organ, an antennal mechanosensory structure previously implicated in near-field sound detection (reviewed in refs 5 and 6). Using enhancer trap lines targeted to different subsets of Johnston's organ neurons[7], and a genetically encoded calcium indicator[8], we show that wind and near-field sound (courtship song) activate distinct populations of Johnston's organ neurons, which project to different regions of the antennal and mechanosensory motor centre in the central brain. Selective genetic ablation of wind-sensitive Johnston's organ neurons in the antenna abolishes wind-induced suppression of locomotion behaviour, without impairing hearing. Moreover, different neuronal subsets within the wind-sensitive population respond to different directions of arista deflection caused by air flow and project to different regions of the antennal and mechanosensory motor centre, providing a rudimentary map of wind direction in the brain. Importantly, sound- and wind-sensitive Johnston's organ neurons exhibit different intrinsic response properties: the former are phasically activated by small, bi-directional, displacements of the aristae, whereas the latter are tonically activated by unidirectional, static deflections of larger magnitude. These different intrinsic properties are well suited to the detection of oscillatory pulses of near-field sound and laminar air flow, respectively. These data identify wind-sensitive neurons in Johnston's organ, a structure that has been primarily associated with hearing, and reveal how the brain can distinguish different types of air particle movements using a common sensory organ.

We observed that *Drosophila* exhibit a rapid and reversible arrest of walking activity under gentle air currents (0.7–1.6 m s^{-1}; Fig. 1a, b and Supplementary Movie 1). This behaviour is also exhibited by wild-caught *Drosophila* species at wind speeds (1.7–2.8 m s^{-1}) within the range measured in their natural habitats[1,2,4] (J. S. Johnston, personal communication; Supplementary Information footnote 1). This behaviour, called wind-induced suppression of locomotion (WISL), was observed in the presence or absence of mechanical startle applied to enhance locomotor activity, before the introduction of air flow (Figs 1b and 3d). Importantly, suppression of locomotion was not observed in response to near-field sound stimuli such as courtship song (280 Hz pulse song, 75–100 dB[9]; Supplementary Fig. 1a).

Recent antennal-gluing experiments have implicated the antenna, and by extension Johnston's organ (JO), in wind sensation in *Drosophila*[3,10]. Surgical removal of the third antennal segment (a3),

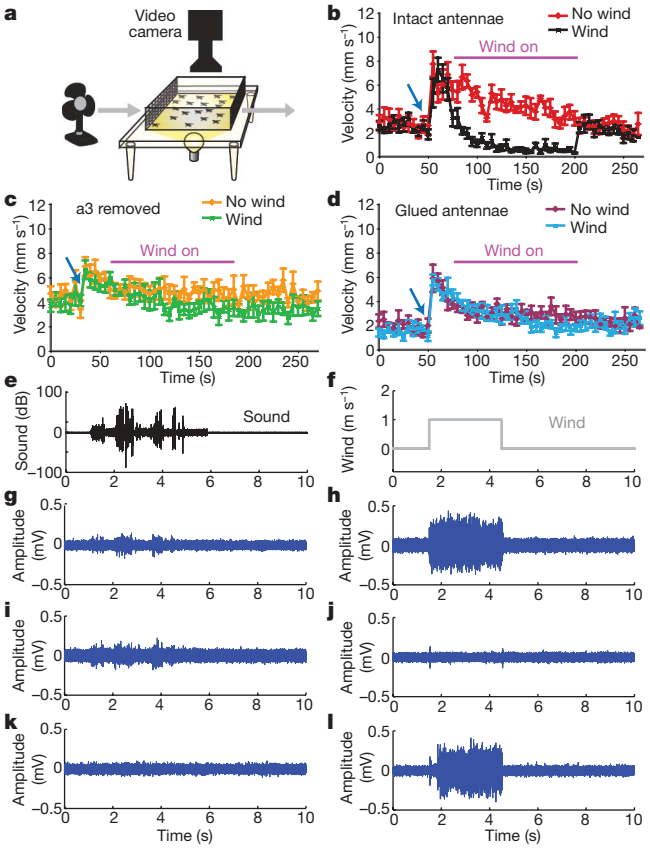

Figure 1 | Behavioural and electrophysiological analyses of wind responses in *Drosophila*. **a**, Schematic illustrating the WISL assay (see Supplementary Methods). **b**, WISL behaviour in Canton-S (CS) flies (Supplementary Movie 1). Data represent mean (± s.e.m.) velocities ($n = 6$). Blue arrow indicates a brief mechanical startle. The 'No wind' versus 'Wind' curves are significantly different ($P = 0.0001$, Kruskal–Wallis analysis of variance (ANOVA)). **c**, **d**, Elimination of WISL by removal of a3 (**c**) or gluing a3 to a2 (**d**). The 'No wind' versus 'Wind' curves are not significantly different ($n = 6$). Data represent mean (± s.e.m). **e–l**, Extracellular recordings of JO neuron responses (blue traces) to sound (**e**) or wind (**f**). **g**, **h**, Response to both sound (**g**) and wind (**h**). **i**, **j**, Response to sound (**i**) but not wind (**j**). **k**, **l**, Response to wind (**l**) but not sound (**k**).

[1]Division of Biology 216-76, [2]Howard Hughes Medical Institute, [3]Division of Engineering and Applied Sciences 136-93, California Institute of Technology, Pasadena, California 91125, USA. [4]Department of Neurobiology and Behavior, SUNY Stony Brook, Stony Brook, New York 11794-5239, USA. [5]Institute of Molecular and Cellular Biosciences, University of Tokyo, Yayoi, Bunkyo-ku, Tokyo 113-0032, Japan. [6]Sensory System Laboratory, Institute of Zoology, University of Cologne, 50923 Cologne, Germany.

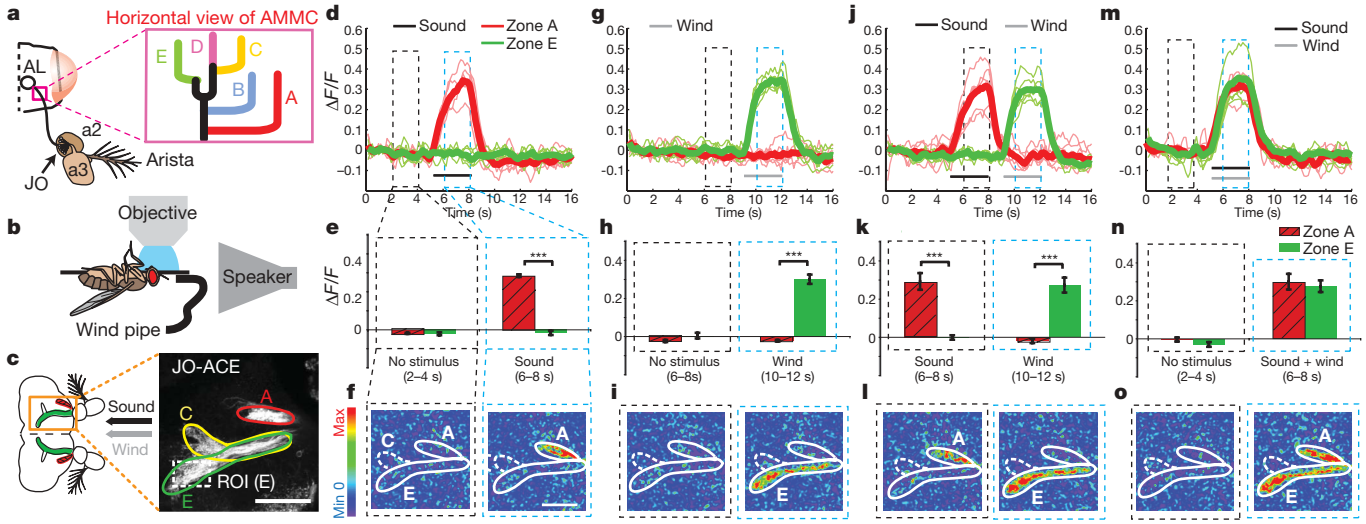

Figure 2 | Calcium imaging reveals distinct populations of wind- and sound-responsive JO neurons. **a–c**, Schematics illustrating location of JO relative to a2 and a3, and five JO neuron axonal terminal zones[7] in the AMMC (**a**), and imaging set-up (**b**). **c**, Zones A, C and E are visualized using a *UAS-mCD8-GFP* reporter. ROI, region of interest for $\Delta F/F$ measurements in zone E. **d–o**, Zones A (red traces, hatched bars) and E (green traces, bars) are activated by sound and wind, respectively, whether presented singly (**d–i**), sequentially (**j–l**) or simultaneously (**m–o**) (see Supplementary Movies 2a–e). Thick traces (**d**, **g**, **j**, **m**) represent the average of the individual (thin) traces ($n = 6$). **e**, **h**, **k**, **n**, Bar graphs indicate the mean (± s.e.m.) integrated $\Delta F/F$ in the time bins (dashed rectangles in **d**, **g**, **j**, **m**; see Methods). $^{***}P < 0.001$ (repeated measure ANOVA and Bonferroni's planned comparisons). **f**, **i**, **l**, **o**, ΔF images of GCaMP activation in zones A and E. Scale bars, 50 μm.

or gluing of a3 to the second antennal segment (a2), both of which cause a functional impairment of JO[11], eliminated WISL (Fig. 1c, d). Genetic ablation of mechanosensory chordotonal neurons using *nanchung-GAL4* (ref. 12) and *UAS-hid* (*head involution defective*, also known as *wrinkled*) a *Drosophila* cell death gene[13], also eliminated WISL (Supplementary Fig. 1b–d). Taken together, these results support the idea that JO is required for WISL, a conclusion confirmed by genetic ablation of specific JO subpopulations (see Fig. 3, later).

To investigate how wind and sound are discriminated by the brain, we first performed extracellular recordings from the antennal nerve[14]. In some electrode placements, spike trains were evoked by both wind (0.3–0.9 m s^{-1}) and courtship song (pulse song; Fig. 1e–h). The short duration of the wind-evoked action potentials (<1 ms) is consistent with neuronal, rather than muscle, action potentials[15]. In other cases, responses were evoked by sound but not wind (Fig. 1i, j; a few spikes were detected at the onset and offset of the wind stimulus), or by wind but not sound (Fig. 1k, l). These results indicate that different axons within the antennal nerve might respond differentially to wind versus sound.

To determine whether distinct subsets of JO neurons are activated by wind versus near-field sound, we performed functional imaging experiments using a genetically encoded calcium sensor (GCaMP-1.3; ref. 8), controlled by different Gal4 enhancer trap lines expressed in JO[7]. These lines identify five major groups of JO axonal projections in the antennal and mechanosensory motor centre (AMMC), called zones A, B, C, D and E (Fig. 2a, inset). Each Gal4 driver labels a subset of zones, but mosaic analysis has revealed that individual JO neurons innervate only one zone[7]. Because it is difficult to distinguish the cell bodies of these five groups of neurons in JO itself, we imaged activity in JO axon terminals in the AMMC, where the five zones are easily discriminated. To do this, we mounted live *Drosophila* in an inverted orientation under a two-photon microscope, while air flow and/or near-field sound were delivered from tubing and a speaker, respectively (Fig. 2b).

Using an enhancer trap line (JO-AB) that selectively labels neurons in zones A and B[7], we observed strong GCaMP activation by courtship song (pulse song; 400 Hz, 90 dB[16]), but not by wind (0.9 m s^{-1}) (Supplementary Fig. 2a–e). Conversely, using a different line (JO-CE) that selectively labels zones C and E[7], we observed responses to air flow, but not to courtship song (Supplementary Fig. 2f–j). To compare directly responses to wind and sound in the same preparation, we used a third line, which labels neurons in zones A, C and E[7] (Fig. 2c). These experiments confirmed that zone A was activated by sound but not by air flow, whereas zone E was activated by air flow but not by sound (Fig. 2d–i and Supplementary Movie 2a, b). The same selective responses were observed when the two stimuli were presented sequentially or simultaneously (Fig. 2j–o and Supplementary Movie 2c, d). Together, these data indicated that JO contains distinct populations of sound- and wind-responsive neurons that project to different regions of the AMMC[7] (Supplementary Information footnote 2).

To determine whether the wind-sensitive JO neurons are also required for WISL behaviour, we genetically ablated these neurons using a toxin, ricin A chain[17]. Because the *JO-CE-GAL4* driver is expressed not only in JO neurons but also in the central brain (Fig. 3a), we used an intersectional strategy to restrict ablation to the antenna using an *eyeless-flippase* (*eyFLP*) tissue-specific recombination system. The specificity of this manipulation was confirmed using an *eyFLP*-dependent mCD8–GFP reporter[18] (Fig. 3b).

Following ablation of JO-C and -E neurons, WISL behaviour was eliminated (Fig. 3g), whereas basal locomotor activity (before wind exposure) and phototaxis behaviour were unaffected (Fig. 3g, i and Supplementary Fig. 3a). Importantly, female flies lacking JO-CE neurons had normal hearing, as evidenced by their unperturbed receptivity to courtship by wild-type males, a behaviour that depends on the females' ability to hear male courtship song. In contrast, females lacking *nanchung*, a gene required for hearing[12], or whose aristae were glued to their head bilaterally[11] (Bi-Gl) exhibited a greatly increased latency to copulation (Fig. 3h, *nan/nan*; Bi-Gl). These data indicate that JO-CE neurons are necessary for WISL behaviour, but dispensable for a hearing-dependent behaviour.

We next investigated the functional significance of the two wind-sensitive JO subpopulations (C and E). Axons innervating zones C and E terminate in lateral versus medial domains of the AMMC, respectively (Fig. 4a–c). When air flow was applied to the front of the head (0°), or at 45°, there was strong activation in zone E and little activation in zone C. Conversely, air flow applied from the rear (180°) activated zone C, and slightly inhibited zone E (Fig. 4d–f and Supplementary Movie 3a–c). Air flow applied to the side of the head

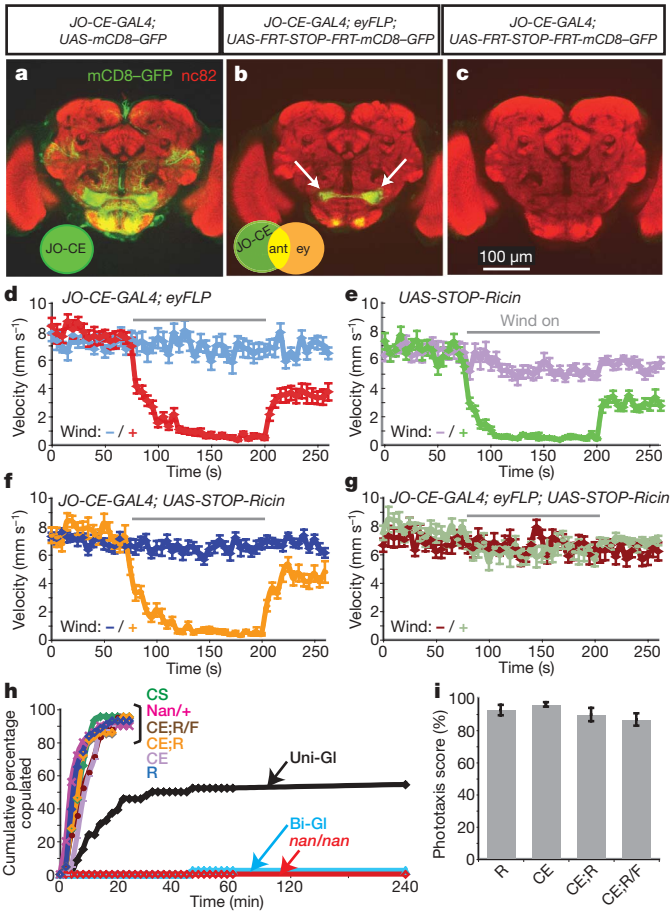

Figure 3 | Ablation of wind-sensitive (C and E) neurons abolishes WISL behaviour. a–c, GFP expression patterns of the indicated genotypes, double-stained with antibodies to GFP (green) and nc82 (red). **a**, Original *JO-CE-GAL4* pattern. **b**, Antennal-restricted *JO-CE-GAL4* pattern using *eyFLP*. Arrows indicate AMMC; underlying structures are gustatory neuron projections to the sub-oesophageal ganglia[7]. **c**, Control for **b** lacking *eyFLP*. **d–g**, WISL analysis. Curves represent mean velocity ± s.e.m. ($n = 15$). **d–f**, Genetic controls show robust WISL. The 'wind−' versus 'wind+' curves are significantly different ($P < 0.0001$). **g**, Ablation of C and E neurons abolishes WISL. **h**, Cumulative percentage of manipulated females copulating with CS males. >90% of all pairs in bracketed conditions exhibited successful copulation within 20 min ($n = 40$–50 pairs). Genotypes: CE;R/F, *JO-CE-GAL4; UAS<STOP<Ricin/eyFLP*; CE;R, *JO-CE-GAL4; UAS<STOP<Ricin*; CE, *JO-CE-GAL4; R, UAS<STOP<Ricin*. Unilateral ('Uni-Gl') or bilateral ('Bi-Gl') gluing of the aristae, or the *nanchung* mutation (*nan/nan*)[12] impaired copulation ($P < 0.0001$). Ablation of JO-CE neurons ('CE;R/F') did not impair either copulation (**h**) or phototaxis (**i**). Phototaxis scores represent mean ± s.e.m. ($n = 7$). *P* values are shown by Kruskal–Wallis ANOVA.

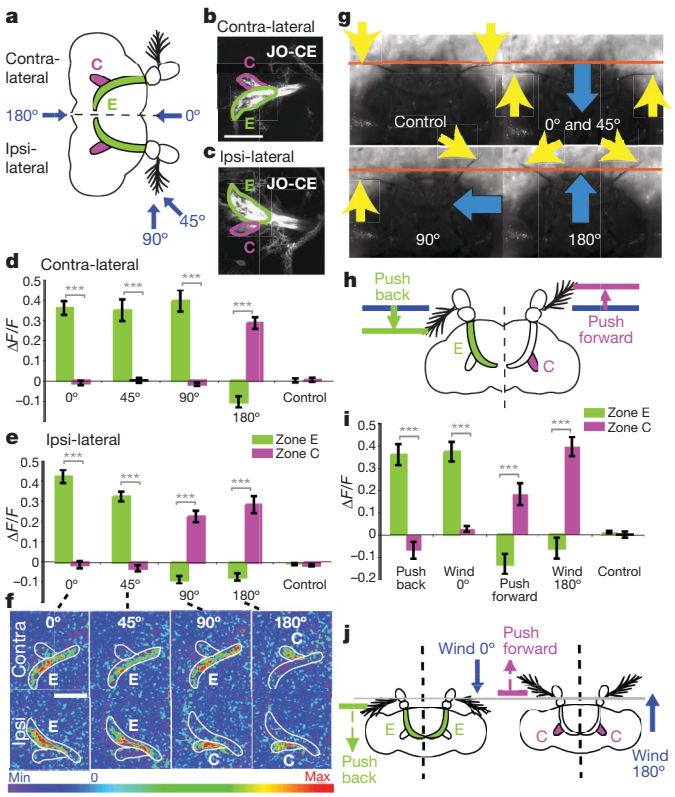

Figure 4 | Wind-direction-sensitivity of zones C versus E. a–c, Schematic (**a**) and mCD8–GFP expression (**b**, **c**) illustrating zones C and E in contra- and ipsi-lateral hemi-brains. Blue arrows indicate wind direction. **d–f**, Average (± s.e.m.) $\Delta F/F$ signals integrated over the stimulus period for zones C and E in the contra- (**d**) and ipsi- (**e**) lateral hemi-brains, and corresponding ΔF images (**f**; see Supplementary Movies 3a–e). **g**, Still frames from video recordings of aristae movements during wind stimulation (Supplementary Movies 4a–e). Yellow arrows indicate aristae position, orange lines denote the rest position ('Control') and blue arrows indicate wind direction. **h**, Schematic illustrating predicted responses of zones C and E to directional, probe-driven aristae displacements. **i**, Responses of the C and E neurons to wind and directional arista displacements. Error bars are s.e.m. **j**, Summary illustrating differential sensitivity of zones C and E to direction of arista displacement. Scale bars, 50 μm. ***$P < 0.0001$ (repeated measures ANOVA and Bonferroni's planned comparisons).

(90°) activated zone C ipsilaterally and zone E contralaterally (Fig. 4d–f, 90°; Supplementary Movie 3d). Thus, zone C and E neurons are differentially sensitive to air flow directionality.

High-magnification video analysis (Supplementary Movie 4a–c) revealed that air flow from different directions moves the aristae either anteriorly or posteriorly (Fig. 4g). We hypothesized that the direction of arista deflection determines whether zone C or E neurons are activated. Arista ablation experiments indicated that the activation of wind-sensitive JO neurons, like that of sound-sensitive JO neurons[11,19], is dependent on this structure (Supplementary Fig. 4). To test the hypothesis directly, we moved the aristae in different directions using a probe controlled by a DC motor (Fig. 4h). Displacing the arista posteriorly with a probe activated the E zone almost as strongly as wind delivered from the front, and weakly inhibited the C zone (Fig. 4i, 'Push back'), whereas displacing it anteriorly activated the C zone and inhibited the E zone (Fig. 4i, 'Push forward'). These data demonstrate that zones C and E are sensitive to different directions of arista deflection (Fig. 4j). This model can explain the asymmetric activation of zones C and E in ipsi- and contral-lateral hemi-brains during wind stimulation from 90° (Fig. 4f, g, 90°), because this stimulus produces opposite deflection of the aristae on the ipsi- and contra-lateral sides of the head (Fig. 4g, 90°, Supplementary Movie 4d). An internal comparison of activity between zones C and E, both within and between each hemi-brain, could provide a basis for computing wind direction[3].

We investigated which stimulus features are responsible for the selective activation of sound- versus wind-sensitive neurons in JO. We first asked whether these two classes of mechanoreceptors are sensitive to different stimulus amplitudes, that is, air particle velocities (v_{air}). A pressure gradient microphone positioned at the antenna[9] yielded a v_{air} of 0.011 m s^{-1} for the 400 Hz sound stimulus played at 90 dB, which maximally activated JO-AB neurons (Fig. 5a). However, this sound stimulus did not activate zone E neurons (Supplementary Fig. 2g), even though these neurons are activated by air flow at a v_{air} as low as 0.005 m s^{-1} (Fig. 5b). Thus, the selectivity of JO-CE and -AB neurons for wind versus sound is not simply due to differences in stimulus magnitude.

We next asked whether JO-AB and -CE neurons might have different intrinsic sensitivities to different types of arista movements by moving

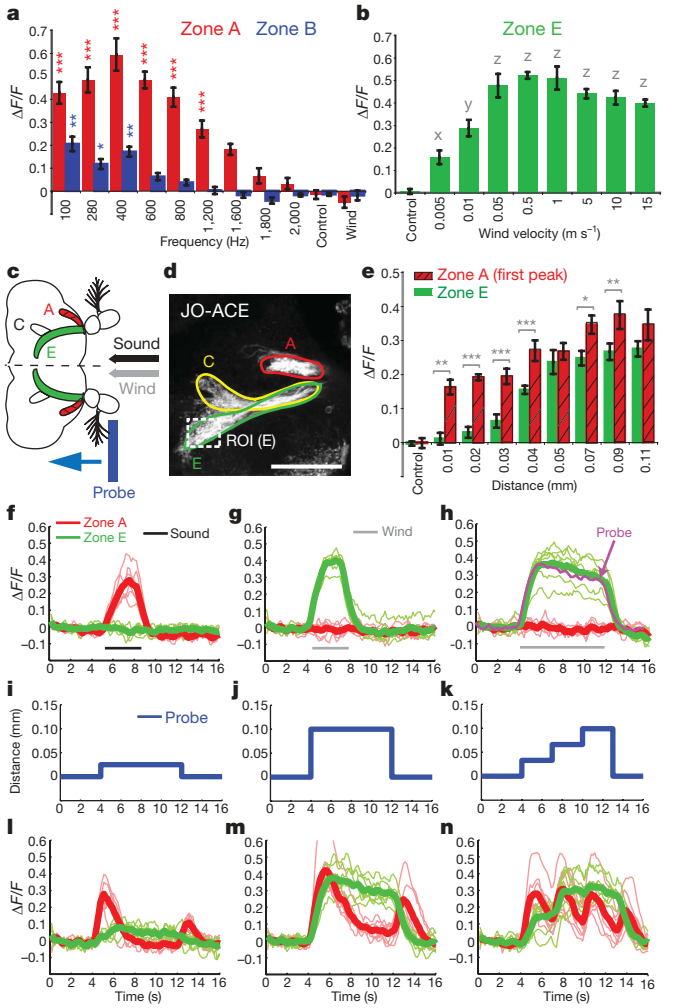

Figure 5 | Wind- and sound-sensitive JO neurons have different intrinsic response properties. **a**, Sensitivity of zones A and B to different sound frequencies (mean ± s.e.m., $n = 6$). ***$P < 0.0001$ (red), *$P < 0.01$ (blue) and **$P < 0.001$ (blue) relative to control. **b**, Sensitivity of zone E to different wind speeds ($n = 5$). Letters (x, y, z) indicate significant differences relative to control (all $P < 0.0001$ except 'x' ($P < 0.001$)). **c–n**, Comparison of sound-, wind- and probe-evoked responses in zones A and E. **c**, **d**, Schematic (**c**) and mCD8–GFP expression (**d**) illustrating zones A, C and E. ROI, region of interest for $\Delta F/F$ measurements in zone E. Scale bar, 50 μm. **e**, Responses of zones A and E to probe-induced arista displacements of different magnitudes. *$P < 0.01$; **$P < 0.001$; ***$P < 0.0001$ (zones A versus E comparisons). All zone A responses, $P < 0.0001$ (relative to control), except for 0.01 mm displacement ($P < 0.001$). All zone E responses ≥0.04 mm displacement, $P < 0.0001$; zone E responses <0.04 mm were not significantly different from control. **f–h**, Sound and wind responses. Thick lines represent average of the individual (thin) traces ($n = 6$). **h**, Superposition of the average responses of zone E to 8 s of wind (green trace) and mechanical probe displacement (magenta trace; see **m**). **i–n**, Responses (**l–n**) of zones A and E to different distances and patterns of probe-induced arista displacement (**i–k**) ($n = 6$). All P values are calculated by repeated measures ANOVA and Bonferroni multiple comparisons.

the aristae in steps of different magnitudes and patterns using a probe controlled by a DC motor (Fig. 5c, d). Sound-sensitive neurons in zone A (Fig. 5f, red traces) were activated by displacements as small as 0.01 mm (Fig. 5e, red hatched bars), whereas wind-sensitive neurons in zone E (Fig. 5g, green traces) were only weakly activated at displacements below 0.04 mm (Fig. 5e, green bars). Thus, zone A neurons have a lower displacement threshold than zone E neurons (see also Fig. 5i, l).

Strikingly, we observed that zone E neurons remained active for as long as the aristae were displaced, whereas zone A neurons were only transiently activated at the onset and offset of probe displacement (Fig. 5j, m). This suggested that zone E neurons might adapt slowly, and therefore respond tonically, whereas zone A neurons might adapt rapidly, and therefore respond phasically. To confirm this, we moved the aristae in three successive steps of 0.033 mm each (total displacement of 0.099 mm; Fig. 5k). Zone A neurons exhibited transient (phasic) responses after each displacement (Fig. 5n, red traces), whereas zone E neurons were tonically activated for the duration of each displacement, and were maximally activated after the second step (Fig. 5n, green traces). These data indicate that JO-AB and JO-CE neurons respond phasically and tonically to arista displacement, with low versus high activation thresholds, respectively (see Supplementary Information footnote 3). Furthermore, zone A neurons were activated by bi-directional movements, whereas zone E neurons were activated only unidirectionally (Fig. 5j, m). These different intrinsic response properties are well matched to the oscillatory arista movements caused by pulses of near-field sound versus uni-directional arista deflections caused by wind. The ability of flies to discriminate wind versus sound using a common sensory organ is thus explained by different populations of JO neurons with different intrinsic response properties, which project to distinct areas of the AMMC.

The identification of different subpopulations of JO neurons with tonic versus phasic response properties illustrates a general and conserved feature of mechanosensation. In mammalian skin, slowly adapting, tonically activated Merkel cells[20] and rapidly adapting, phasically activated Meissner's corpuscles[21] are used for different types of light-touch sensation. In *Drosophila*, these two properties have been adapted to detect different types of bulk air particle movements by different subsets of JO neurons. In the accompanying paper[22], the authors demonstrate, using complementary imaging methods, that zone AB neurons are activated by sound and required for hearing. They also show that zone CE neurons are required for the behavioural response to gravity (negative gravitaxis), a force that could also produce static deflections of the arista, albeit of a smaller magnitude than those produced by wind (Supplementary Information footnote 4).

The data presented here indicate that JO is not simply a hearing organ[6] but also mediates wind detection, in a direction-sensitive manner. Wind-activated neurons in JO are, moreover, required for an innate behavioural response to wind. The function of WISL in nature is not clear. Field studies have suggested that wind is a major environmental factor affecting the dispersal of wild *Drosophila* populations[1,2,4]. WISL may have evolved to control population dispersal, and thereby maintain genetic homogeneity[1,2]. Alternatively, WISL may represent a defence mechanism that serves to protect individual flies from injury, or to prevent dispersal from food resources. Identification of the sensory neurons that mediate WISL opens the way to a systematic analysis of the genes and neural circuitry that underlie this robust, innate behavioural response to wind.

METHODS SUMMARY

Behavioural assay. Twenty flies were used for each WISL trial. A standard WISL trial lasts for 270 s. During the first 55 s, the flies' baseline locomotor activity was recorded. Where indicated, at $t = 55$ s, a brief mechanical stimulus was applied to transiently increase the flies' locomotor activity. Air flow exposure was then initiated at $t = 80$ s, and terminated at $t = 200$ s.

Electrophysiology. Sample preparation and electrophysiological recordings from JO axons were performed as described[14].

Calcium-response imaging. Flies were anaesthetized in a plastic vial on ice for 15−20 s, and then gently inserted into a hole of a thin plastic rectangular plate. After stabilizing the fly with a small drop of wax (55 °C), the proboscis and the area surrounding the proboscis were surgically removed, in a saline bath, to expose the ventral side of the brain. The preparation was then mounted on a microscope in an inverted orientation for calcium-response imaging. The antennae were kept intact and dry throughout the exposure to different stimuli (sound, wind and mechanical probe displacement).

Detailed descriptions of fly stocks, the WISL behavioural apparatus and assay, courtship and phototaxis assays, antennal manipulations, electrophysiology, calcium-response imaging and sample preparation, sound and wind stimuli and statistical methods are provided in the Supplementary Methods.

Full Methods and any associated references are available in the online version of the paper at www.nature.com/nature.

Received 25 November 2008; accepted 29 January 2009.

1. Johnston, J. & Templeton, A. in *Ecological Genetics and Evolution* (eds Barker, J. S. F. & Starmer, W. T.) 241–256 (Academic, 1982).
2. Johnston, J. & Heed, W. Dispersal of desert-adapted *Drosophila*: the saguaro-breeding *D. nigrospiracula*. *Am. Nat.* **110,** 629–651 (1976).
3. Budick, S. A., Reiser, M. B. & Dickinson, M. H. The role of visual and mechanosensory cues in structuring forward flight in *Drosophila melanogaster*. *J. Exp. Biol.* **210,** 4092–4103 (2007).
4. Richardson, R. & Johnston, J. Behavioral components of dispersal in *Drosophila mimica*. *Oecologia* **20,** 287–299 (1975).
5. Caldwell, J. C. & Eberl, D. F. Towards a molecular understanding of *Drosophila* hearing. *J. Neurobiol.* **53,** 172–189 (2002).
6. Kernan, M. J. Mechanotransduction and auditory transduction in *Drosophila*. *Pflügers Arch.* **454,** 703–720 (2007).
7. Kamikouchi, A., Shimada, T. & Ito, K. Comprehensive classification of the auditory sensory projections in the brain of the fruit fly *Drosophila melanogaster*. *J. Comp. Neurol.* **499,** 317–356 (2006).
8. Nakai, J., Ohkura, M. & Imoto, K. A high signal-to-noise Ca^{2+} probe composed of a single green fluorescent protein. *Nature Biotechnol.* **19,** 137–141 (2001).
9. Göpfert, M. C. & Robert, D. The mechanical basis of *Drosophila* audition. *J. Exp. Biol.* **205,** 1199–1208 (2002).
10. Mamiya, A. *et al.* Neural representations of airflow in *Drosophila* mushroom body. *PLoS ONE* **3,** e4063 (2008).
11. Manning, A. Antennae and sexual receptivity in *Drosophila melanogaster* females. *Science* **158,** 136–137 (1967).
12. Kim, J. *et al.* A TRPV family ion channel required for hearing in *Drosophila*. *Nature* **424,** 81–84 (2003).
13. Wang, S. L. *et al.* The *Drosophila* caspase inhibitor DIAP1 is essential for cell survival and is negatively regulated by HID. *Cell* **98,** 453–463 (1999).
14. Eberl, D. F., Hardy, R. W. & Kernan, M. J. Genetically similar transduction mechanisms for touch and hearing in *Drosophila*. *J. Neurosci.* **20,** 5981–5988 (2000).
15. Tanouye, M. A. & Wyman, R. J. Motor outputs of giant nerve fiber in *Drosophila*. *J. Neurophysiol.* **44,** 405–421 (1980).
16. Bennet-Clark, H. C. Acoustics of insect song. *Nature* **234,** 255–259 (1971).
17. Moffat, K. G. *et al.* Inducible cell ablation in *Drosophila* by cold-sensitive ricin A chain. *Development* **114,** 681–687 (1992).
18. Wong, A. M., Wang, J. W. & Axel, R. Spatial representation of the glomerular map in the *Drosophila* protocerebrum. *Cell* **109,** 229–241 (2002).
19. Ewing, A. W. The antenna of *Drosophila* as a 'love song' receptor. *Physiol. Entomol.* **3,** 33–36 (1978).
20. Ikeda, I. *et al.* Selective phototoxic destruction of rat Merkel cells abolishes responses of slowly adapting type I mechanoreceptor units. *J. Physiol. (Lond.)* **479,** 247–256 (1994).
21. Hoffmann, J. N., Montag, A. G. & Dominy, N. J. Meissner corpuscles and somatosensory acuity: the prehensile appendages of primates and elephants. *Anat. Rec. A Discov. Mol. Cell. Evol. Biol.* **281,** 1138–1147 (2004).
22. Kamikouchi, A. *et al.* The neural basis of *Drosophila* gravity-sensing and hearing. *Nature* doi:1010.1038/nature07810 (this issue).

Supplementary Information is linked to the online version of the paper at www.nature.com/nature.

Acknowledgements We thank U. Heberlein and F. Wolf for hosting a sabbatical that led to the discovery of WISL; J. S. Johnson for helpful discussions; L. Zelnik, M. Reiser and P. Perona for creating locomotor tracking software; D. Eberl and J. Hall for *D. melanogaster* courtship song recordings; G. Maimon for making fly holders for imaging experiments; M. Roy for building behavioral chambers for WISL and female receptivity assays; H. Inagaki for *JO-CE-GAL4;eyFLP* flies; B. Hay for *UAS-hid* flies; D. Berdnik for *UAS-FRT-STOP-FRT-Ricin* flies; M. Dickinson for anemometers and discussions; J. L. Anderson for advice on fluid mechanics; M. Göpfert for providing a pressure gradient microphone; M. Konishi for advice and use of laboratory facilities; and G. Mosconi for laboratory management. D.J.A. is an Investigator of the Howard Hughes Medical Institute. This work was supported in part by NSF grant EF-0623527.

Author Contributions S.Y. and D.J.A. designed experiments, S.Y. carried out all experiments reported in this paper and D.J.A. and S.Y. wrote the manuscript. A.W. wrote Matlab programs for $\Delta F/F$ measurements and mechanical probe actuation, B.J.F. assisted with computational filtering of song stimuli, H.D. assisted with computational and statistical analysis of data, M.J.K. provided facilities and support for electrophysiological experiments, and A.K. and K.I. provided Gal4 lines.

Author Information Reprints and permissions information is available at www.nature.com/reprints. Correspondence and requests for materials should be addressed to D.J.A. (mancusog@caltech.edu) or S.Y. (yorozu@caltech.edu).

METHODS

Fly stocks. Flies carrying *JO-ACE*, *JO-CE* and *JO-AB* were described previously[7]. *UAS-GCaMP*[23,24] and *UAS-mCD8-GFP* flies were obtained from Y. Wang and R. Axel, *UAS-FRT-STOP-FRT-Ricin* flies[25] were obtained from D. Berdnik, *JO-CE-GAL4; eyFLP* flies were obtained from H. Inagaki, Canton-S flies from J. Dubnau, and *UAS-hid* flies from B. Hay. Flies were maintained on corn meal and molasses food at 25 °C on a (12/12) light–dark cycle.

WISL behavioural apparatus. The WISL assay was performed in a $6 \times 6 \times 1.5$ cm transparent acrylic plastic box (WISL chamber), which has air flow inputs and outputs (1 cm diameter) on two of the four vertical sides of the box. The input tubing carries air flow from a tank containing breathable air, connected to a flow regulator. The output tubing allows the air flow to escape from the box, and is connected to a flow meter that measures the speed of the air flow. The WISL chamber was mounted on a transparent plastic table and was trans-illuminated with a fluorescent light from underneath. A video camera (Sony, DCR-HC40 NTSC) was set up above the WISL chamber to record the flies' locomotor activity.

WISL assay protocol. Twenty flies per trial were sorted 36–48 h before testing, using nitrogen gas or cold anaesthesia. On the testing day, 20 flies were aspirated into the WISL chamber and allowed to acclimate for 7–8 min just before initiation of the trial. A standard WISL trial lasted for 270 s. Flies were given a brief mechanical stimulation (5 manual strikes on the table that the WISL chamber was mounted on) at 55 s, and air flow exposure began at 80 s and ended at 120 s. Locomotor activity was recorded at ten frames per second and average velocity was computed using custom software written in Matlab (MathWorks Inc.).

Courtship (female receptivity) assay. Naive Canton-S males and virgin females of the genotype of interest were collected immediately after eclosion, using nitrogen or CO_2 gas anaesthesia. Naive males were individually housed whereas virgin females were group-housed for six days until the test day. Single naive Canton-S male and a single virgin female of the genotype of interest were placed in a mating chamber ($1 \times 1 \times 0.4$ cm square chamber), and the time at which a successful copulation occurred was recorded for each mating pair. Successful copulation typically lasts 15–25 min.

Phototaxis assay. Forty flies per trial were sorted 48 h before testing, using nitrogen or CO_2 gas anaesthesia. On the test day, 40 flies were tapped into the elevator of a T-maze and allowed to rest for one minute in a dark. Next, the elevator was lowered to the choice point where flies were given one minute to make a choice between a dark tube and a tube illuminated with a 40 W fluorescent light, positioned approximately 20 cm away. The phototaxis response was analysed by calculating the performance index (PI) using the following formula: $PI = [(2 \times COR) - 1] \times 100$, where COR = (number of flies that chose the illuminated tube/total number of flies). PI = 0 indicates an equal distribution of flies between the dark and illuminated tubes. PI = 100% indicates that all flies chose the illuminated tube.

Antenna manipulations. To test the role of JO in wind detection, a3 segments were surgically removed using a pair of forceps, 48 h before the WISL testing. For the antennal gluing experiment, a small drop of ultraviolet-activated glue was placed at the junction between the a2 and a3 segments bilaterally, and cured with an ultraviolet lamp for 3–5 s, 48 h before the testing. For the mechanical probe antennal displacement experiment, a sharpened tungsten needle was used to move the aristae in different directions and different patterns. The probe was mounted on a DC motor/controller (LTA-HS and SMC100CC, Newport), which was controlled by custom Matlab software (MathWorks Inc.). To push the aristae backward, the probe was positioned anterior to the aristae; conversely, to push the aristae forward, the probe was positioned posterior to the aristae. In the 'push back' (and 'push forward') conditions, the aristae were pushed backward (or forward) in a single increment of varying distances (0.01, 0.02, 0.025, 0.03, 0.04, 0.05, 0.07, 0.09 or 0.11 mm), held for 8 s in the displaced position and then returned to the original position. In another experiment, the aristae was pushed backwards in three successive steps of 0.033 mm (a total of 0.099 mm), held in place for 2.9 s after each successive step, and then returned to the original position. In all conditions, the probe and aristae movements were verified using a video camera (GE680, Proscillica) that was set up underneath the fly preparation mounted on the microscope stage as described previously.

Electrophysiology. Extracellular recordings from JO axons were recorded at the a1/a2 joint using a tungsten or glass electrode (0.5 MΩ) as described previously[14] in a sound-proof chamber. Pulse-song segments of recorded *D. melanogaster* courtship song (provided by J. Hall[26] and D. Eberl) were used as the sound stimulus and an air flow rate between 0.3 and 0.9 m s^{-1} was used as the wind stimulus.

Calcium-response imaging and sample preparation. Flies were anaesthetized in a plastic vial on ice for ~15–20 s, and were then gently inserted into a hole of a thin plastic rectangular plate. Small drops of wax (55 °C) were applied to prevent the fly from moving out from the hole. After the fly was stabilized in the plastic hole, the preparation was oriented in an upside-down position (see Fig. 2b). The proboscis, ventral part of thorax and abdomen, and legs were protruding from the upper side of the horizontal plane of the plastic, while the rest of the fly head (including the antennae, but excluding the proboscis), thorax and dorsal part of abdomen were protruding from the bottom side of the horizontal plane of the plastic. In a saline bath, the proboscis was cut off and the area surrounding the proboscis was surgically removed to expose the ventral side of the brain. Fat and air sacs were gently removed to give a clear view of the brain. For calcium-response imaging, the water immersion objective lens (×40, NA = 0.8, Olympus) was lowered near the exposed brain, while the underside of the plastic specimen mount, which contained the intact antennae, was kept dry and exposed to wind and sound stimuli.

Sound stimuli used in these experiments were recorded segments (provided by J. Hall[26] and D. Eberl) of the pulse-song portion of *D. melanogaster* courtship song, played at 75–100 dB at the aristae using a loudspeaker (ProMonitor 800 loudspeaker, Definitive Technology) and amplifier (P.A. amplifier, Radioshack) and were measured using a digital sound meter (DSM-325, Mannix). We tested the frequency tuning of zones A and B using narrowband signals derived from the original pulse-song. The original pulse-song was filtered to set the centre of the frequency spectrum at a desired frequency between 100 and 2,000 ± 200 Hz (using the Fourier transformation).

Wind stimuli used in imaging experiments were delivered at speeds between 0.005 and 15 m s^{-1}. Wind speed was controlled by a flow regulator (mass flow meters and controllers, Smart Trak series 100, Sierra Instrument Inc.) and was measured using an anenometer (Testo-435, Testo GmbH & Co.). VClamp software (Pairie Technology) was used to control all aspects of sound and wind stimuli used in the imaging experiments.

All imaging was performed on an Ultima two-photon laser scanning microscope (Prairie Technology). Live images were acquired at 6.1 frames per second using an Olympus ×40 (NA = 0.8) water immersion objective at 128×128 resolution with an imaging wavelength at 925 nm. GCaMP responses were quantified using custom software written in MatLab. The relative change in fluorescence intensity ($\Delta F/F$) was computed by first calculating the average pixel values in the region of interest during the experimental period and applying a three-frame moving average smoothing function. This average fluorescence value, F_{av}, was then converted to $\Delta F/F$ using the formula $\Delta F/F = (F_{av} - F_0)/F_0$, where F_0 is the baseline fluorescence value, measured as the average of frames 2–9. Average $\Delta F/F$ for a specific stimulus period was compared between different JO neuron zones to test for statistical significance by repeated-measure ANOVA.

23. Wang, J. W., Wong, A. M., Flores, J., Vosshall, L. B. & Axel, R. Two-photon calcium imaging reveals an odor-evoked map of activity in the fly brain. *Cell* **112,** 271–282 (2003).
24. Wang, Y. *et al.* Stereotyped odor-evoked activity in the mushroom body of Drosophila revealed by green fluorescent protein-based Ca^{2+} imaging. *J. Neurosci.* **24,** 6507–6514 (2004).
25. Berdnik, D., Chihara, T., Couto, A. & Luo, L. Wiring stability of the adult *Drosophila* olfactory circuit after lesion. *J. Neurosci.* **26,** 3367–3376 (2006).
26. Wheeler, D. A., Fields, W. L. & Hall, J. C. Spectral analysis of *Drosophila* courtship songs: *D. melanogaster*, *D. simulans*, and their interspecific hybrid. *Behav. Genet.* **18,** 675–703 (1988).